Acta Crystallographica Section F
Structural Biology and Crystallization Communications
ISSN 1744-3091

Preliminary X-ray crystallographic studies of UDP-glucose-4-epimerase from *Aspergillus nidulans*

Sean A. Dalrymple,[a] Inder Sheoran,[a] Susan G. W. Kaminskyj[b] and David A. R. Sanders[a]*

[a]Department of Chemistry, University of Saskatchewan, 110 Science Place, Saskatoon, Saskatchewan S7N 5C9, Canada, and [b]Department of Biology, University of Saskatchewan, 112 Science Place, Saskatoon, Saskatchewan S7N 5E2, Canada

Correspondence e-mail: david.sanders@usask.ca

Received 7 March 2011
Accepted 31 May 2011

UDP-glucose-4-epimerase (GALE) from *Aspergillus nidulans* was overexpressed in *Escherichia coli*, purified *via* His-tag affinity chromatography and cocrystallized with UDP-galactose using the microbatch method. The crystals diffracted to 2.4 Å resolution using synchrotron radiation on the Canadian Light Source 08ID-1 beamline. Examination of the data with *d*TREK* revealed non-merohedral twinning, from which a single lattice was ultimately extracted for processing. The final space group was found to be *C*2, with unit-cell parameters $a = 66.13$, $b = 119.15$, $c = 161.42$ Å, $\beta = 98.48^\circ$. An initial structure solution has been obtained *via* molecular replacement employing human GALE (PDB entry 1hzj) as a template model.

1. Introduction

UDP-glucose-4-epimerase (GALE), also known as UDP-galactose-4-epimerase, is an NAD^+-dependent enzyme that is responsible for reversibly inverting the 4′-hydroxyl configuration of UDP-galactose to form UDP-glucose in a wide variety of species (Fig. 1; Allard *et al.*, 2001; Holden *et al.*, 2003). GALE catalyzes the final step in the Leloir pathway for normal galactose metabolism and impairment of the enzyme in humans results in type III galactosemia (Lai *et al.*, 2009; Thoden *et al.*, 2001*b*). Although most of the structural work to date has centered around the homodimers found in the *Escherichia coli* and human forms (Thoden *et al.*, 2001*a*, 2002), a limited number of GALE structures from additional species, including yeast and protists, have appeared in the literature (Shaw *et al.*, 2003; Thoden *et al.*, 2005).

In contrast, little is known structurally with regard to GALE from fungal sources. Pathogenic fungi, namely *Aspergillus* spp., have gained notoriety for posing an increased threat to human health, particularly in immunocompromised individuals, in recent decades (Pfaller & Diekema, 2007). There are many challenges in treating fungal pathogens within human hosts owing to the close evolutionary relationship which exists between these eukaryotic systems (Baldauf *et al.*, 2000). In addition to the limited number of viable drug targets within fungi, most treatments have reduced potency owing to either host toxicity or, more recently, the emergence of drug resistance (Odds *et al.*, 2003). The evolution of fungal drug resistance, complicated by the therapeutically intractable nature of these pathogens, is of serious clinical concern and has recently been reviewed in the literature (Cowen, 2008). Given the many issues associated with treating fungal diseases, research into the development of new classes of drugs, very few of which have reached clinical trials in recent

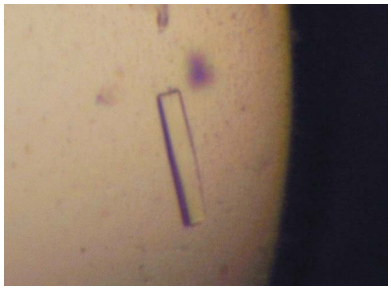

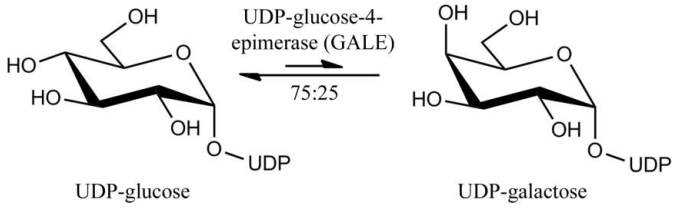

Figure 1
The interconversion reaction catalyzed by UDP-glucose-4-epimerase (GALE).

decades, is clearly warranted (Slavin, 2008). Currently, antifungal drugs which block cell-wall synthesis, such as the echinocandins, are believed to be the most promising candidates for clinical treatments (Cappelletty & Eiselstein-McKitrick, 2007).

As GALE catalyzes the production of precursor building blocks for fungal lipopolysaccharide (LPS) biosynthesis, explicitly UDP-galactose, the enzyme and its corresponding pathway are of interest from a drug-target perspective (Pedersen & Turco, 2003). Given that GALE exhibits interspecies variation at both the structural and functional levels, targetable differences between GALE of the host and pathogen can be employed for rational drug design. In this context, our laboratory has been conducting biochemical and structural studies on GALE from *A. nidulans*, with the goal of elucidating the structure–function relationship responsible for its catalytic role in galactose metabolism. The *A. nidulans* GALE sequence was initially identified by homology to human GALE and consists of 372 amino acids with a molecular weight of 40.6 kDa (El-Ganiny *et al.*, 2010). In order to identify exploitable differences for drug targeting, detailed structural characterization of *A. nidulans* GALE is required.

2. Methods and materials

2.1. Expression and purification

Plasmid construction and DNA transformation of *A. nidulans* GALE was conducted according to previously published methods (El-Ganiny *et al.*, 2010). Overexpression of N-terminal pHISTEV-GALE was carried out in BL21-Gold (DE3) (Novagen) cells, which were cultured at 310 K and 250 rev min^{-1} in LB medium containing 50 µg ml^{-1} kanamycin. Expression was induced by the addition of 1 m*M* IPTG at an OD_{600} of 0.5 and the cells were then grown for an additional 24 h at 288 K and 250 rev min^{-1}. The cells were harvested and subsequently resuspended in lysis buffer (buffer *A*) consisting of 0.1 *M* NaCl and 0.05 *M* NaH_2PO_4 pH 8. After addition of lysozyme (2 µ*M*) and a catalytic quantity of DNAse, the cells were sonicated and the ruptured cell debris was removed *via* centrifugation at 27 000*g* for 30 min at 277 K. The supernatant was passed through a 0.22 µm filter (Amicon) prior to loading onto a Protino Ni–IDA packed column (Macherey-Nagel) pre-equilibrated with buffer *B* (0.4 *M* NaCl and 0.05 *M* NaH_2PO_4 pH 8) at 295 K. Prior to elution, the column was washed with ten column volumes of buffer *B* and GALE was eluted with a ten-column-volume linear gradient from 0 to 250 m*M* imidazole in 0.05 *M* NaH_2PO_4 pH 8 containing 0.4 *M* NaCl at a flow rate of 5 ml min^{-1}. A single peak centered at 130 m*M* imidazole was observed in the elution profile for His_6-tagged GALE and the corresponding fractions were analyzed by SDS–PAGE. The GALE-containing fractions were then pooled and concentrated with the aid of a 30K centrifugal filter device (Amicon) before being dialyzed against 25 m*M* Tris pH 8. The final protein concentration, as determined by the Bradford assay, was adjusted to 15 mg ml^{-1} for crystallization trials.

2.2. Crystallization

Commercial crystallization kits (Qiagen) were initially employed for broad screening of conditions to produce X-ray-quality single crystals by the microbatch method at 277 K. Crystallization drops were formed by combining equal volumes (1.2 µl) of protein solution and precipitant solution prior to layering with paraffin oil (Hampton Research) in an effort to slow vapour diffusion. Screening trials were also conducted in the presence of substrate, specifically 10 m*M* UDP-galactose, which was incubated with GALE for 1 h prior to setup. Positive hits from the initial screening conditions shared two common features: crystals grew from solutions containing polyethylene glycol (PEG) 3350 and within the pH range 7.5–8.5. Three similar conditions from the PACT screening kit (Qiagen) produced X-ray-quality crystals in the presence of UDP-galactose: condition Nos. 75 [20%(*w*/*v*) PEG 3350, 0.1 *M* Bis-Tris propane pH 7.5, 0.2 *M* sodium fluoride], 84 [20%(*w*/*v*) PEG 3350, 0.1 *M* Bis-Tris propane pH 7.5, 0.2 *M* sodium malonate] and 86 [20%(*w*/*v*) PEG 3350, 0.1 *M* Bis-Tris propane pH 8.5, 0.2 *M* sodium bromide]. Ultimately, hexagonal rod-shaped crystals from PACT condition No. 75, which grew to 0.1 × 0.1 × 0.4 mm over a period of two weeks, were employed for X-ray diffraction studies (Fig. 2). Although larger crystals with dimensions of up to 0.25 × 0.25 × 0.5 mm could be obtained using an extended growth period, such crystals suffered from poor-quality diffraction.

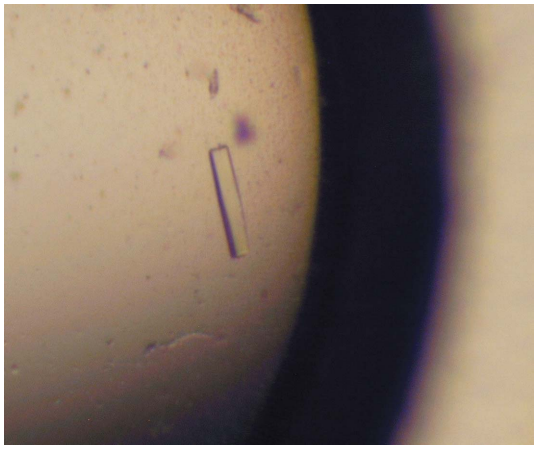

Figure 2
Crystals of the *A. nidulans* GALE complex grown using the microbatch method under paraffin oil at 277 K with approximate dimensions of 0.1 × 0.1 × 0.45 mm.

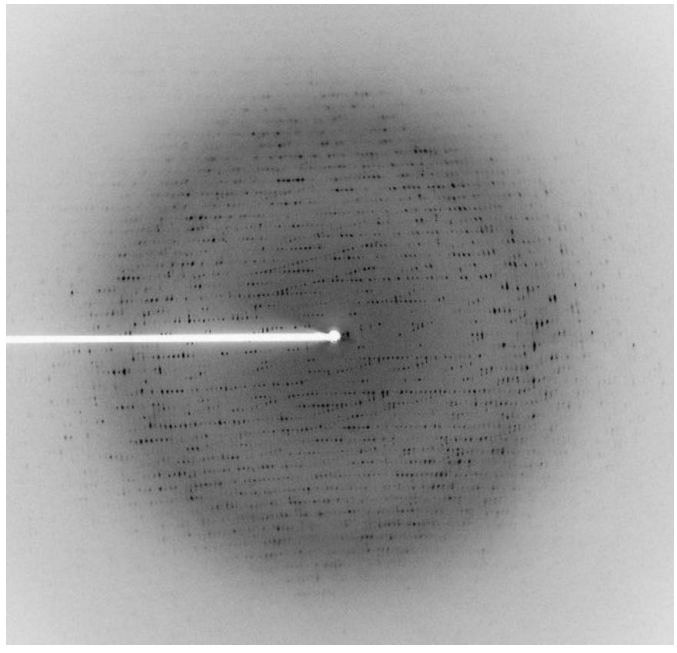

Figure 3
Representative diffraction image for the *A. nidulans* GALE complex showing the presence of a second lattice which was selectively omitted from subsequent data processing with *d*TREK*.

Table 1
Data-collection statistics for *A. nidulans* GALE crystals.

Values in parentheses are for the highest resolution shell.

Beamline	08ID-1, CLS
Wavelength (Å)	0.9790
Temperature (K)	100
Space group	*C*2
Unit-cell parameters (Å, °)	a = 66.13, b = 119.15, c = 161.42, $\alpha = \gamma = 90$, β = 98.48
Resolution (Å)	36.71–2.40 (2.49–2.40)
Observed reflections	340066
Unique reflections	47599
Completeness (%)	98.4 (98.1)
Multiplicity	7.14 (7.33)
$\langle I/\sigma(I)\rangle$	5.5 (2.0)
$R_{\rm merge}$†	0.161 (0.687)

† $R_{\rm merge} = \sum_{hkl}\sum_i |I_i(hkl) - \langle I(hkl)\rangle| / \sum_{hkl}\sum_i I_i(hkl)$, where $I_i(hkl)$ is the measured intensity and $\langle I(hkl)\rangle$ is the average intensity over symmetry-equivalent reflections.

2.3. Data collection and processing

In order to cryoprotect the crystals from radiation damage, the samples were quickly transferred into mother-liquor solution containing 25% glycerol. After a few seconds, the crystals were mounted onto a CryoLoop (Hampton Research) and flash-cooled in liquid nitrogen. Subsequently, all data collections were carried out at 100 K under a stream of nitrogen gas. A data set for wild-type *A. nidulans* GALE was collected to a resolution of 2.4 Å on the Canadian Light Source (CLS) 08ID-1 beamline using a MAR Mosaic MX-300 CCD detector. A total of 360 images were collected with an exposure of 1 s and 1.0° oscillation at a crystal-to-detector distance of 250 mm. Examination of the diffraction patterns from multiple data sets revealed the consistent presence of nonmerohedral twinning from a weaker second lattice (Fig. 3).

3. Results and discussion

The overexpression protocol led to 80 mg pure protein being obtained from 1 l LB culture after purification. With regard to the nonmerohedral twinning, the stronger lattice was extracted for data processing in *d*TRE*K by employing a cutoff whereby data with intensities of less than eight times the standard deviation were rejected from integration and scaling (Pflugrath, 1999). Relevant data-collection statistics for the *A. nidulans* GALE complex are presented in Table 1. *A. nidulans* GALE crystals grown in the presence of UDP-galactose belonged to the monoclinic space group *C*2, with unit-cell parameters a = 66.13, b = 119.15, c = 161.42 Å, β = 98.48°. After processing with *d*TREK*, the structure was solved by molecular replacement *via MrBUMP* (Keegan & Winn, 2007) within the *CCP*4 package (Winn *et al.*, 2011). The initial solution was determined by *MOLREP* (Vagin & Teplyakov, 1997) employing human GALE (PDB entry 1hzj; Thoden *et al.*, 2001*a*), which shares 51% sequence identity with the *A. nidulans* protein, as the template model. Examination of the best solution (R factor of 52.1%) revealed the presence of three distinct monomers per asymmetric unit, corresponding to a Matthews coefficient of 2.51 Å^3 Da^{-1} and a solvent content of 51.06%. Subsequently, the molecular-replacement solution was inspected using *Coot* (Emsley & Cowtan, 2004), which confirmed the absence of deleterious steric clashes with symmetry-related GALE molecules. Additionally, the characteristic homodimer interface that was previously observed in both the *E. coli* (Thoden *et al.*, 1996) and human (Thoden *et al.*, 2000) forms was also evident in the model. The unit cell consists of one homodimer and a monomer that forms a crystallographic dimer. While electron density for the cofactor, namely NAD(H), was clearly evident in each of the monomers, the difference map also revealed substrate density exceeding 3σ corresponding to a UDP-sugar moiety within each of the monomer active sites. Initial restrained refinement was carried out in *PHENIX* (Adams *et al.*, 2010) using *phenix.refine* (Afonine *et al.*, 2005), which showed a marked improvement of the model, resulting in an R factor of 32.9% and an $R_{\rm free}$ of 37.1%. Further refinement and additional model building are currently in progress and structural details will be described in a separate paper.

We would like to thank the staff of macromolecular beamline 08ID-1, Canadian Light Source (CLS), Saskatoon, Saskatchewan, Canada for their technical assistance during data collection. This work was supported by a CIHR–Regional Partnership Program grant to DARS and SGWK. Additionally, SAD would like to acknowledge funding from SHRF through a Postdoctoral Research Fellowship. The research described in this paper was performed at the CLS, which is supported by NSERC, the National Research Council of Canada, the Canadian Institutes of Health Research, the Province of Saskatchewan, Western Economic Diversification Canada and the University of Saskatchewan.

References

Adams, P. D. *et al.* (2010). *Acta Cryst.* D**66**, 213–221.
Afonine, P. V., Grosse-Kunstleve, R. W. & Adams, P. D. (2005). *CCP4 Newsl.* **42**, contribution 8.
Allard, S. T., Giraud, M. F. & Naismith, J. H. (2001). *Cell. Mol. Life Sci.* **58**, 1650–1665.
Baldauf, S. L., Roger, A. J., Wenk-Siefert, I. & Doolittle, W. F. (2000). *Science*, **290**, 972–977.
Cappelletty, D. & Eiselstein-McKitrick, K. (2007). *Pharmacotherapy*, **27**, 369–388.
Cowen, L. E. (2008). *Nature Rev. Microbiol.* **6**, 187–198.
El-Ganiny, A. M., Sheoran, I., Sanders, D. A. & Kaminskyj, S. G. (2010). *Fungal Genet. Biol.* **47**, 629–635.
Emsley, P. & Cowtan, K. (2004). *Acta Cryst.* D**60**, 2126–2132.
Holden, H. M., Rayment, I. & Thoden, J. B. (2003). *J. Biol. Chem.* **278**, 43885–43888.
Keegan, R. M. & Winn, M. D. (2007). *Acta Cryst.* D**63**, 447–457.
Lai, K., Elsas, L. J. & Wierenga, K. J. (2009). *IUBMB Life*, **61**, 1063–1074.
Odds, F. C., Brown, A. J. & Gow, N. A. (2003). *Trends Microbiol.* **11**, 272–279.
Pedersen, L. L. & Turco, S. J. (2003). *Cell. Mol. Life Sci.* **60**, 259–266.
Pfaller, M. A. & Diekema, D. J. (2007). *Clin. Microbiol. Rev.* **20**, 133–163.
Pflugrath, J. W. (1999). *Acta Cryst.* D**55**, 1718–1725.
Shaw, M. P., Bond, C. S., Roper, J. R., Gourley, D. G., Ferguson, M. A. & Hunter, W. N. (2003). *Mol. Biochem. Parasitol.* **126**, 173–180.
Slavin, M. A. (2008). *Int. J. Infect. Dis.* **12**, e12.
Thoden, J. B., Frey, P. A. & Holden, H. M. (1996). *Protein Sci.* **5**, 2149–2161.
Thoden, J. B., Henderson, J. M., Fridovich-Keil, J. L. & Holden, H. M. (2002). *J. Biol. Chem.* **277**, 27528–27534.
Thoden, J. B., Sellick, C. A., Timson, D. J., Reece, R. J. & Holden, H. M. (2005). *J. Biol. Chem.* **280**, 36905–36911.
Thoden, J. B., Wohlers, T. M., Fridovich-Keil, J. L. & Holden, H. M. (2000). *Biochemistry*, **39**, 5691–5701.
Thoden, J. B., Wohlers, T. M., Fridovich-Keil, J. L. & Holden, H. M. (2001*a*). *J. Biol. Chem.* **276**, 15131–15136.
Thoden, J. B., Wohlers, T. M., Fridovich-Keil, J. L. & Holden, H. M. (2001*b*). *J. Biol. Chem.* **276**, 20617–20623.
Vagin, A. & Teplyakov, A. (1997). *J. Appl. Cryst.* **30**, 1022–1025.
Winn, M. D. *et al.* (2011). *Acta Cryst.* D**67**, 235–242.